



Lattice Dynamics of Oxyfluoride $\text{Rb}_2\text{KMoO}_3\text{F}_3$

A. S. Krylov , S. N. Sofronova , E. M. Kolesnikova , A. N. Vtyurin & L. I. Isaenko

To cite this article: A. S. Krylov , S. N. Sofronova , E. M. Kolesnikova , A. N. Vtyurin & L. I. Isaenko (2012) Lattice Dynamics of Oxyfluoride $\text{Rb}_2\text{KMoO}_3\text{F}_3$, *Ferroelectrics*, 441:1, 52-60, DOI: [10.1080/00150193.2012.743791](https://doi.org/10.1080/00150193.2012.743791)

To link to this article: <https://doi.org/10.1080/00150193.2012.743791>



Published online: 19 Dec 2012.



Submit your article to this journal [↗](#)



Article views: 83



View related articles [↗](#)

Lattice Dynamics of Oxyfluoride $\text{Rb}_2\text{KMoO}_3\text{F}_3$

A. S. KRYLOV,¹ S. N. SOFRONOVA,^{1,*} E. M. KOLESNIKOVA,¹
A. N. VTYURIN,¹ AND L. I. ISAENKO²

¹L.V. Kirensky Institute of Physics SB RAS, 660036, Krasnoyarsk, Russia

²V.S. Sobolev Institute of Geology and Mineralogy SB RAS, 630090,
Novosibirsk, Russia

The complete Raman spectra of oxyfluoride $\text{Rb}_2\text{KMoO}_3\text{F}_3$ were obtained. At $T \approx 185$ K phase transitions were found. Lattice dynamics of disordered structures of the investigated compound was simulated, and “soft” vibrational modes were found in the calculated spectrum.

Keywords Oxyfluorides; lattice dynamics; Raman measurements

I. Introduction

The oxyfluoride $\text{Rb}_2\text{KMoO}_3\text{F}_3$ belongs to a large class of elpasolite-type crystals with the general formula $\text{A}_2\text{BMO}_3\text{F}_3$ ($\text{A}, \text{B} = \text{NH}_4, \text{Na}, \text{K}, \text{Rb}, \text{Cs}$; $\text{M} = \text{Mo}, \text{W}$). Depending on the ratio of ionic radii R_A и R_B , as well as nature of atom M, the symmetry $Fm\bar{3}m$ of high temperature phase of these compounds could remain stable down to the temperature of liquid helium [1–6] or become distorted as a result of one [1–5, 7] or two phase transitions [1–6, 8–10]. For example, in spite of very close values of ionic radii of Mo atoms ($R_{\text{Mo}} = 0.073$ nm) and W ($R_{\text{W}} = 0.074$ nm), elpasolite $\text{Rb}_2\text{KMoO}_3\text{F}_3$ undergoes phase transition [11], while elpasolite $\text{Rb}_2\text{KW}\text{O}_3\text{F}_3$ retains cubic symmetry and does not exhibit any phase transitions [12]. It should be noted that the high-temperature cubic phase is realized in these compounds due to disordering of the F/O anions in the crystal. Depending on the arrangement of F/O atoms, the local configuration of the octahedric MO_3F_3 groups can be either a mer- (symmetry C_{2v}), or the fac- (symmetry C_{3v}). It has been shown in Ref. [13] that in $\text{Rb}_2\text{KMoO}_3\text{F}_3$ these octahedra are predominantly in the fac-configuration.

It is known that oxyfluoride $\text{Rb}_2\text{KMoO}_3\text{F}_3$ undergoes an order-disorder structural phase transition at $T = 195$ K [11], which is far from the tricritical point at the heating mode of the sample. However, the symmetry of the low-temperature phase is still unknown.

The purpose of this paper is to present results of experimental and theoretical investigations of $\text{Rb}_2\text{KMoO}_3\text{F}_3$ lattice dynamics and anions ordering by Raman technique in the framework of generalized Gordon-Kim model and to make an attempt to explain the mechanism of the phase transition in this crystal.

II. Raman Measurements

The unpolarized Raman spectra of the nonoriented $\text{Rb}_2\text{KMoO}_3\text{F}_3$ single crystal were obtained using a Horiba Jobin Yvon T64000 Raman spectrometer. We used $1.5 \times 1.5 \times 1.5$ mm sized sample no. 7, which was described in Ref. [11]. A single-mode Ar^+ laser with wavelength $\lambda = 514.5$ nm was used as an excitation light source. The radiation power at the sample was 7 mW.

To extract quantitative information on the spectral parameters of the experimental data, the spectra were deconvolved into individual lines. At lower frequencies (< 150 cm^{-1}) damped harmonic oscillator [14] was used as a model of the line shape function. Lorentzian [15] contour was used above 150 cm^{-1} .

Figure 1 shows the complete experimental Raman spectra of oxyfluoride $\text{Rb}_2\text{KMoO}_3\text{F}_3$ at room temperature and at $T = 7$ K.

Earlier [16] higher frequency part of the spectrum, which contains the fully symmetric stretching mode of Mo-O bonds of anionic octahedrons, was obtained with lower resolution (2 cm^{-1}) and fitted by a single Lorentz contour. In this study, this part of the spectrum was obtained with better resolution (0.7 cm^{-1}); analysis of the spectra has shown that this spectral region contains two lines (Fig. 2), though this mode in the cubic phase is nondegenerate. Temperature dependence of the relative intensity of these two lines is shown in the inset in Fig. 2.

Figure 3 shows the complete temperature dependence of Raman spectra of the crystal $\text{Rb}_2\text{KMoO}_3\text{F}_3$. It is seen that at $T \approx 185$ K a phase transition occurs, and, according to the typical drastic changes of the spectral parameters, this phase transition is of the first order. Major changes occur in the fully symmetric vibrations of Mo-O and Mo-F, as well as in the external lattice vibrations region. Doubling of the line numbers can be clearly seen in the range of Mo-O vibrations and in the region of external lattice vibrations below the phase transition. This may indicate an increase in the unit cell volume of at least two times.

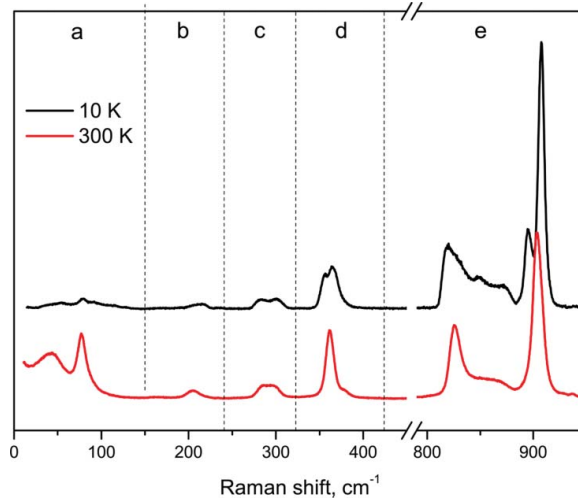


Figure 1. Raman spectrum of oxyfluoride $\text{Rb}_2\text{KMoO}_3\text{F}_3$ at room temperature ($T = 300$ K) and at $T = 10$ K: (a) – the external lattice vibration range; (b) – the range of O-Mo-F bendings; (c) – the range of O-Mo-O bendings; (d) – the range of Mo-F stretchings; (e) – the range of Mo-O stretchings [1] (Figure available in color online).

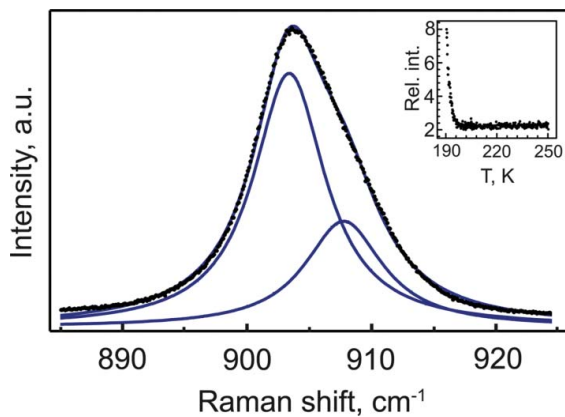


Figure 2. Part of the spectrum, which contains the fully symmetric stretching mode of Mo-O, fitted by two Lorentz contours (inset – relative intensity of these two lines) (Figure available in color online).

The temperature dependences of the frequencies of totally symmetric vibrations of Mo-O and Mo-F are shown in Fig. 4. The discontinuous jump of frequencies in the vicinity of the phase transition point is clearly seen: the frequency of the oxygen mode increases below the transition temperature, while the frequency of the fluorine line decreases. These

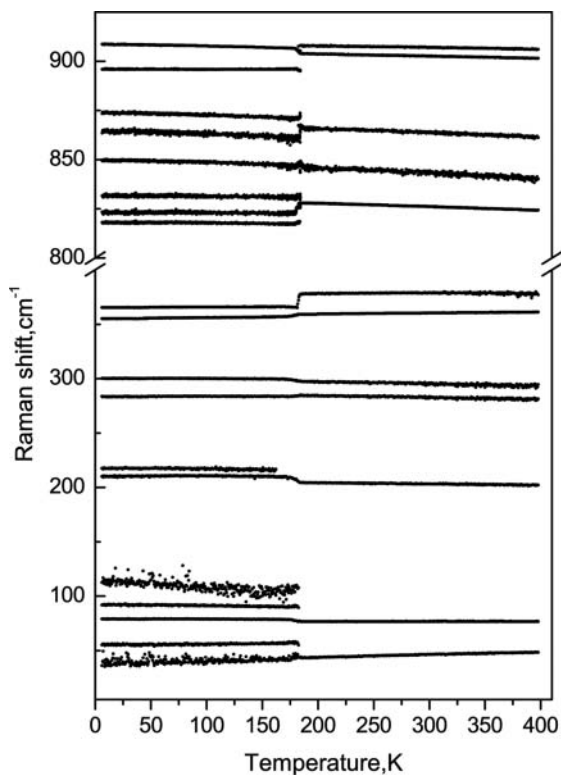


Figure 3. Temperature dependence of Raman spectra of oxyfluoride $\text{Rb}_2\text{KMoO}_3\text{F}_3$.

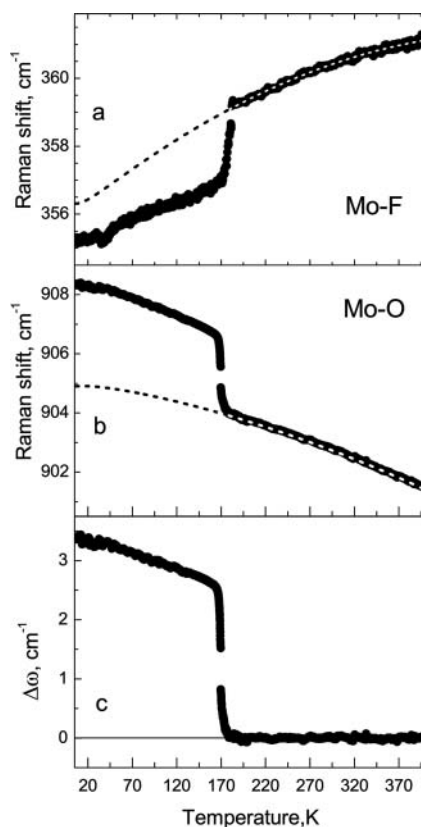


Figure 4. (a), (b) – temperature dependences of fully symmetric vibrations Mo-F and Mo-O (dash curves – theoretical approximations); (c) – temperature dependence of order parameter (the difference of experimental Mo-O frequency and the approximated data).

dependences were approximated taking into account the three- and four-phonon interactions due to lattice inharmonicity in the absence of phase transitions [17]. According to Ref. [18], the frequency shift $\Delta\omega$ of the fully symmetric high-frequency vibrations (the difference of experimental frequency and the approximated data) is proportional to the square of the order parameter. The corresponding dependence shows typical behavior of the first order phase transitions far from the tricritical point.

The widths of fully symmetric vibrations Mo-O and Mo-F also experience anomalies at the phase transition temperature (Fig. 5). The obtained dependences are non-typical for an ordered solids. There is a pronounced anomalous λ -shaped behavior of the linewidth of the fully symmetric vibrations of Mo-O and, to a lesser extent, of the totally symmetric vibrations of Mo-F. Such anomalous dependence of the characteristic of the order-disorder phase transitions may be caused by the growth of order parameter fluctuations near the transition point [19].

In ordered elpasolite at liquid helium temperatures the linewidths of anionic octahedral fully symmetric vibrations tend to the values of $\sim 1\text{--}3\text{ cm}^{-1}$ [20–22]. Totally symmetric vibration 908 cm^{-1} in this case can serve as a parameter related to the degree of ordering of the octahedra $[MoO_3F_3]^{3-}$. Bigger ($\approx 6\text{ cm}^{-1}$) values of these linewidths, as compared with

Figure 5. Temperature dependences of the frequency and the full width of fully symmetric Mo–O vibration (open circles – FWHM; solid circles – Raman shift).

well ordered elpasolites, prove that the total ordering of the octahedrons is not happening even at liquid helium temperatures.

III. Lattice Dynamics Simulation by Generalized Gordon-Kim Model

In the present study, the generalized Gordon-Kim model has been used for lattice dynamics simulations of elpasolite $\text{Rb}_2\text{KMoO}_3\text{F}_3$ [23].

In the high-temperature cubic phase F/O anions are disordered. As a consequence of this disorder, each octahedron in the unit cell can be located in 20 states equally (8 states of trigonal symmetry C_{3v} and 12 states of the orthorhombic symmetry C_{2v}). The authors of Ref. [13] have shown that anionic octahedron $[\text{MoO}_3\text{F}_3]^{3-}$ has a predominantly trigonal symmetry (fac-conformation); therefore here we considered fac-conformations only.

To simulate lattice disorder, a cubic unit cell of elpasolite type was chosen, that contained four formula units ($Z = 4$). Then the dynamical matrix (its eigenvalues are the frequencies of lattice normal modes) was calculated for all possible orderings of F/O octahedra in the fac-configuration of the cell (4 octahedrons in the unit cell, and each of them can be in eight equiprobable orientations – that gives 4096 structures). The lattice parameters were cubic and determined by minimizing the total energy of the crystal ($a_{\text{cub}} = 8.427 \text{ \AA}$). The lattice frequencies of a disordered crystal were calculated as the eigenvalues of the “average” dynamical matrix. Unstable modes of vibration of the atoms, obtained in the calculation are presented in Table 1. Simulated spectrum includes “soft” modes related both to the center of the Brillouin zone of the cubic cell, and to the boundary points of the Brillouin zone. Condensation of the last ones would induce a structural phase transition with unit cell multiplication. The displacements of the atoms corresponding to the “soft” mode eigenvectors are presented in Table 1.

Table 1
Calculated eigenvectors of the “soft” modes ($Z = 4$).

Atom	Coordinates ($a; b; c$)	141i(2)	141i(2)	139i(2)	98i(2)	60i(2)	59i(2)	44i(2)	33i(2)
Rb	(0.25;0.25;0.25)	(x;-y;0)	(-x;-y;0)	(0;0;z)	(x;0;0)	(0;0;z)	(x;0;0)	(-x;0;0)	(0;0;0)
Rb	(0.25;0.25;0.75)	(x;-y;0)	(-x;-y;0)	(0;0;-z)	(x;0;0)	(0;0;-z)	(x;0;0)	(x;0;0)	(0;0;0)
Rb	(0.25;0.75;0.25)	(-x;y;0)	(x;y;0)	(0;0;z)	(x;0;0)	(0;0;-z)	(-x;0;0)	(-x;0;0)	(0;0;0)
Rb	(0.25;0.75;0.75)	(-x;y;0)	(x;y;0)	(0;0;-z)	(x;0;0)	(0;0;z)	(-x;0;0)	(x;0;0)	(0;0;0)
Rb	(0.75;0.25;0.25)	(-x;y;0)	(x;y;0)	(0;0;z)	(x;0;0)	(0;0;-z)	(-x;0;0)	(x;0;0)	(0;0;0)
Rb	(0.75;0.25;0.75)	(-x;y;0)	(x;y;0)	(0;0;-z)	(x;0;0)	(0;0;z)	(-x;0;0)	(-x;0;0)	(0;0;0)
Rb	(0.75;0.75;0.25)	(x;-y;0)	(-x;-y;0)	(0;0;z)	(x;0;0)	(0;0;-z)	(x;0;0)	(x;0;0)	(0;0;0)
Rb	(0.75;0.75;0.75)	(x;-y;0)	(-x;-y;0)	(0;0;-z)	(x;0;0)	(0;0;z)	(x;0;0)	(-x;0;0)	(0;0;0)
K	(0.5;0.5;0.5)	(-x;y;-z)	(-x;-y;z)	(0;0;z)	(x;0;0)	(0;y;0)	(0;y;0)	(0;0;z)	(-x;0;0)
K	(0;0;0.5)	(-x;y;z)	(-x;-y;-z)	(0;0;-z)	(x;0;0)	(0;-y;0)	(0;y;0)	(0;0;-z)	(x;0;0)
K	(0;0.5;0)	(x;-y;z)	(x;y;-z)	(0;0;z)	(x;0;0)	(0;-y;0)	(0;-y;0)	(0;0;z)	(x;0;0)
K	(0.5;0;0)	(x;-y;-z)	(x;y;z)	(0;0;-z)	(x;0;0)	(0;y;0)	(0;-y;0)	(0;0;-z)	(-x;0;0)
Mo	(0;0;0)	(-x;y;-z)	(-x;-y;z)	(x;0;0)	(x;0;0)	(0;y;0)	(0;y;0)	(0;0;-z)	(x;0;0)
Mo	(0.5;0.5;0)	(-x;y;z)	(-x;-y;-z)	(-x;0;0)	(x;0;0)	(0;-y;0)	(0;-y;0)	(0;0;-z)	(-x;0;0)
Mo	(0.5;0;0.5)	(x;-y;z)	(x;y;-z)	(x;0;0)	(x;0;0)	(0;-y;0)	(0;-y;0)	(0;0;-z)	(-x;0;0)
Mo	(0;0.5;0.5)	(x;-y;-z)	(x;y;z)	(-x;0;0)	(x;0;0)	(0;y;0)	(0;-y;0)	(0;0;-z)	(x;0;0)
O/F	(0.208;0;0)	(x;-y;z)	(x;y;-z)	(-x;0;0)	(x;0;0)	(0;y;0)	(0;-y;0)	(0;0;-z)	(-x;0;0)
O/F	(0;0.208;0)	(x;-y;z)	(x;y;-z)	(-x;0;0)	(x;0;0)	(0;y;0)	(0;-y;0)	(0;0;-z)	(-x;0;0)
O/F	(0;0;0.208)	(x;-y;z)	(x;y;-z)	(-x;0;0)	(x;0;0)	(0;y;0)	(0;-y;0)	(0;0;-z)	(-x;0;0)
O/F	(0.708;0.5;0)	(x;-y;-z)	(x;y;z)	(x;0;0)	(x;0;0)	(0;-y;0)	(0;y;0)	(0;0;z)	(x;0;0)
O/F	(0.5;0.708;0)	(x;-y;-z)	(x;y;z)	(x;0;0)	(x;0;0)	(0;y;0)	(0;-y;0)	(0;0;z)	(x;0;0)
O/F	(0.5;0.5;0.208)	(x;-y;-z)	(x;y;z)	(x;0;0)	(x;0;0)	(0;-y;0)	(0;y;0)	(0;0;-z)	(-x;0;0)
O/F	(0.708;0;0.5)	(-x;y;-z)	(-x;-y;z)	(-x;0;0)	(x;0;0)	(0;-y;0)	(0;-y;0)	(0;0;-z)	(x;0;0)
O/F	(0.5;0.208;0.5)	(-x;y;-z)	(-x;-y;z)	(-x;0;0)	(x;0;0)	(0;y;0)	(0;y;0)	(0;0;-z)	(-x;0;0)

(Continued on next page)

Table 1
Calculated eigenvectors of the “soft” modes ($Z = 4$). (Continued)

“Soft” modes and corresponding eigenvectors										
Atom	Coordinates ($a; b; c$)	141i(2)	141i(2)	139i(2)	98i(2)	60i(2)	59i(2)	44i(2)	33i(2)	
O/F	(0.5;0;0.708)	(-x;y;-z)	(-x;-y;z)	(-x;0;0)	(x;0;0)	(0;-y;0)	(0;-y;0)	(0;0;z)	(-x;0;0)	
O/F	(0.208;0.5;0.5)	(-x;y;z)	(-x;-y;-z)	(x;0;0)	(x;0;0)	(0;y;0)	(0;-y;0)	(0;0;z)	(-x;0;0)	
O/F	(0;0.708;0.5)	(-x;y;z)	(-x;-y;-z)	(x;0;0)	(x;0;0)	(0;-y;0)	(0;y;0)	(0;0;z)	(x;0;0)	
O/F	(0;0.5;0.708)	(-x;y;z)	(-x;-y;-z)	(x;0;0)	(x;0;0)	(0;y;0)	(0;-y;0)	(0;0;-z)	(x;0;0)	
O/F	(0.792;0;0)	(x;-y;z)	(x;y;-z)	(-x;0;0)	(x;0;0)	(0;y;0)	(0;y;0)	(0;0;-z)	(-x;0;0)	
O/F	(0;0.792;0)	(x;-y;z)	(x;y;-z)	(-x;0;0)	(x;0;0)	(0;y;0)	(0;y;0)	(0;0;-z)	(x;0;0)	
O/F	(0;0;0.792)	(x;-y;-z)	(x;y;z)	(x;0;0)	(x;0;0)	(0;-y;0)	(0;y;0)	(0;0;z)	(x;0;0)	
O/F	(0.292;0.5;0)	(x;-y;-z)	(x;y;z)	(x;0;0)	(x;0;0)	(0;y;0)	(0;y;0)	(0;0;z)	(x;0;0)	
O/F	(0.5;0.292;0)	(x;-y;-z)	(x;y;z)	(x;0;0)	(x;0;0)	(0;y;0)	(0;y;0)	(0;0;z)	(-x;0;0)	
O/F	(0.5;0.5;0.792)	(x;-y;-z)	(x;y;z)	(x;0;0)	(x;0;0)	(0;-y;0)	(0;y;0)	(0;0;z)	(-x;0;0)	
O/F	(0.292;0;0.5)	(-x;y;-z)	(-x;-y;z)	(-x;0;0)	(x;0;0)	(0;-y;0)	(0;-y;0)	(0;0;-z)	(x;0;0)	
O/F	(0.5;0.792;0.5)	(-x;y;-z)	(-x;-y;z)	(-x;0;0)	(x;0;0)	(0;y;0)	(0;-y;0)	(0;0;-z)	(-x;0;0)	
O/F	(0.5;0;0.292)	(-x;y;-z)	(-x;-y;z)	(-x;0;0)	(x;0;0)	(0;-y;0)	(0;-y;0)	(0;0;-z)	(-x;0;0)	
O/F	(0.792;0.5;0.5)	(-x;y;z)	(-x;-y;-z)	(x;0;0)	(x;0;0)	(0;y;0)	(0;-y;0)	(0;0;z)	(-x;0;0)	
O/F	(0;0.292;0.5)	(-x;y;z)	(-x;-y;-z)	(x;0;0)	(x;0;0)	(0;-y;0)	(0;-y;0)	(0;0;z)	(x;0;0)	
O/F	(0;0.5;0.292)	(-x;y;z)	(-x;-y;-z)	(x;0;0)	(x;0;0)	(0;y;0)	(0;-y;0)	(0;0;z)	(x;0;0)	

IV. Conclusions

In the crystal $Rb_2KMoO_3F_3$ the first order order-disorder phase transition at $T \approx 185$ K was revealed in a cooling mode of the sample. According to the theoretical and experimental results, it may be suggested that this phase transition is mainly associated with molecular octahedrons $[MoO_3F_3]^{3-}$ and accompanied by unit cell multiplication. At the present time, the question of ordering F/O octahedral group and its role in the structural phase transition remains open. Further study is required to establish the symmetry of the low-temperature phase and to understand the nature of the phase transition.

References

1. M. Couzi, V. Rodriguez, J. P. Chaminade, M. Fouad, and J. Ravez, Raman scattering in ferroelectric materials with composition $A_2BMO_3F_3$ ($A, B = K, Rb, Cs$ for $r_{A+} \geq r_{B+}$ and $M = Mo, W$). *Ferroelectrics* **80**, 109–112 (1980).
2. V. D. Fokina, I. N. Flerov, G. V. Gorev, M. S. Molokeev, A. D. Vasiliev, and M. N. Laptsh, Effect of cationic substitution on ferroelectric and ferroelastic phase transitions in oxyfluorides $A_2A'WO_3F_3$ ($A, A': K, NH_4, Cs$). *Ferroelectrics* **347**, 60–64 (2007).
3. G. Peraudeau, J. Ravez, P. Haggemuller, and H. Arend, Study of phase transitions in $A_3MO_3F_3$ compounds ($A = K, Rb, Cs; M = Mo, W$). *Solid State Commun.* **27**, 591–593 (1978).
4. J. Ravez, G. Peraudeau, H. Arend, S. C. Abrahams, and P. Haggemuller, A new family of ferroelectric materials with composition $A_2BMO_3F_3$ ($A, B = K, Rb, Cs$, for $r_{A+} \geq r_{B+}$ and $M = Mo, W$). *Ferroelectrics* **26**, 767–769 (1980).
5. G. Peraudeau, J. Ravez, and H. Arend, Etude des transitions de phases des composés $Rb_2KMO_3F_3$, $Cs_2KMO_3F_3$ et $Cs_2RbMO_3F_3$ ($M = Mo, W$). *Solid State Commun.* **27**, 515–518 (1978).
6. A. S. Krylov, A. N. Vtyurin, V. D. Fokina, S. V. Goryainov, and A. G. Kocharova, Raman spectroscopic study of the phase transitions in the $Cs_2NH_4WO_3F_3$ oxyfluoride. *Phys. Solid State* **48** (6), 1064–1066 (2006).
7. A. S. Krylov, S. V. Goryainov, A. N. Vtyurin, S. N. Krylova, S. N. Sofronova, N. M. Laptash, T. B. Emelina, V. N. Voronov, and S. V. Babushkin, Raman scattering study of temperature and hydrostatic pressure phase transitions in Rb_2KTiOF_5 crystal. *J. Raman Spectrosc.* **43** (4), 577–582 (2012).
8. V. V. Atuchin, L. I. Isaenko, V. G. Kesler, Z. S. Lin, M. S. Molokeev, A. P. Yelisseyev, and S. A. Zhurkov, Exploration on anion ordering, optical properties and electronic structure in $K_3WO_3F_3$ elpasolite. *J. Solid State Chem.* **187**, 159–164 (2012).
9. A. Ekimov, A. Krylov, A. Vtyurin, A. Ivanenko, N. Shestakov, and A. Kocharova, Vibrational spectroscopy studies of temperature phase transitions in $K_3WO_3F_3$. *Ferroelectrics* **401**, 168–172 (2010).
10. G. Peraudeau, J. Ravez, A. Tressaud, P. Haggemuller, and H. Arend, Les transitions de phase de l'oxyfluoride $Rb_3MoO_3F_3$. *Solid State Commun.* **23**, 543–546 (1977).
11. E. I. Pogorel'tsev, E. V. Bogdanov, M. S. Molokeev, V. N. Voronov, L. I. Isaenko, S. A. Zhurkov, N. M. Laptash, M. V. Gorev, and I. N. Flerov, Thermodynamic properties and structure of oxyfluorides $Rb_2KMoO_3F_3$ and $K_2NaMoO_3F_3$. *Phys. Solid State* **53** (6), 1202–1211 (2011).
12. A. V. Kartashev, M. S. Molokeev, L. I. Isaenko, S. A. Zhurkov, V. D. Fokina, M. V. Gorev, and I. N. Flerov, Heat capacity and structure of $Rb_2KMeO_3F_3$ ($Me: Mo, W$) elpasolites. *Solid State Sci.* **14**, 166–170 (2012).
13. A. A. Udovenko and N. M. Laptash, Orientational disorder in crystals of $(NH_4)_3MoO_3F_3$ and $(NH_4)_3WO_3F_3$. *Acta Crystallogr. B* **64**, 305–311 (2008).
14. L. H. Hoang, N. T.M. Hien, W. S. Choi, Y. S. Lee, K. Taniguchi, T. Arima, S. Yoon, X. B. Chen, and I. S. Yang, Temperature-dependent Raman scattering study of multiferroic $MnWO_4$. *J. Raman Spectrosc.* **41**, 1005–1010 (2009).

15. V. K. Malinovsky, A. M. Pugachev, and N. V. Surovtsev, Low-frequency Raman scattering study of the ferroelectric phase transition in the DKDP crystal. *Phys. Solid State* **50** (6), 1137–1143 (2008).
16. A. S. Krylov, E. M. Merkusheva, A. N. Vtyurin, and L. I. Isaenko, Raman spectroscopic study of the lattice dynamics in the $\text{Rb}_2\text{KMoO}_3\text{F}_3$ oxyfluoride. *Phys. Solid State* **54** (6), 1275–1280 (2012).
17. C. Ramkumar, K. P. Jain, and S. C. Abbi, Raman-scattering probe of anharmonic effects due to temperature and compositional disorder in III-V binary and ternary alloy semiconductors. *Phys. Rev. B: Condens. Matter* **53** (20), 13672–13681 (1996).
18. J. Petzelt and V. Dvorak, Changes of infrared and Raman spectra induced by structural phase transitions: I. General considerations. *J. Phys. C: Solid State Phys.* **9**, 1571–1586 (1976).
19. M. Musso, F. Matthai, D. Keutel, and K. Oehme, Isotropic Raman line shapes near gas–liquid critical points: The shift, width, and asymmetry of coupled and uncoupled states of fluid nitrogen. *J. Chem. Phys.* **116** (18), 8015–8027 (2002).
20. G. Baldinozzi, Ph. Sciau, and A. Bulou, Analysis of the phase transition sequence of the elpasolite (ordered perovskite) $\text{Pb}_2\text{MgTeO}_6$. *J. Phys. Condens. Matter* **9**, 10531–10544 (1997).
21. S. N. Krylova, A. N. Vtyurin, A. Bulou, A. S. Krylov, and N. G. Zamkova, Lattice dynamics and Raman scattering spectrum of elpasolite Rb_2KScF_6 : Comparative analysis. *Phys. Solid State* **46** (7), 1311–1319 (2004).
22. A. S. Krylov, S. N. Krylova, A. N. Vtyurin, N. V. Surovtsev, S. V. Adishev, V. N. Voronov, and A. S. Oreshonkov, Raman spectra and phase transitions in Rb_2KInF_6 elpasolite. *Crystallogr. Rep.* **56** (1), 18–23 (2011).
23. N. G. Zamkova, V. I. Zinenko, O. V. Ivanov, E. G. Maksimov, and S. N. Sofronova, Lattice dynamics calculation of the ionic crystals with ion dipole and quadrupole deformations perovskite structure oxides. *Ferroelectrics* **283**, 49–60 (2003).